# Ceramic Pebble Production from the Break-Up of a Molten Laminar Jet

Oliver Leys[1]*, Patrick Waibel[2], Jörg Matthes[2], Regina Knitter[1]
[1]Institute for Applied Materials (IAM), [2]Institute for Automation and Applied Informatics (IAI)
Karlsruhe Institute of Technology (KIT), Karlsruhe, Germany
*Corresponding author: oliver.leys@kit.edu

**Abstract**
Lithium rich ceramic pebbles are required for tritium breeding in future fusion reactors. The pebbles will be installed in the form of pebble beds in the wall of the reactor and upon irradiation, will generate tritium to be used as a fuel for the fusion reaction. A melt-based process has been developed at the Karlsruhe Institute of Technology, which produces pebbles from the break-up of a molten jet. Synthesis powders are heated in a platinum alloy crucible to approximately 1400 °C, after which a pressure is applied to the system, forming a jet through a nozzle on the underside of the crucible. The jet then breaks up while entering a cooling tower, where the droplets are solidified using a liquid nitrogen spray system. The produced pebbles generally have sizes ranging from 250 to 1250 µm.

Recent research has focused on the optimisation of the jet break-up stage of the production process. An image processing algorithm (specifically written for this process) was used in conjunction with a high-speed camera to determine various jet and droplet characteristics shortly after ejection from the nozzle. Initial studies focused on the effects of the operating pressure and more recently, a method for applying desired frequencies to induce the jet break-up at high temperatures was developed. It has been shown that under controlled conditions, it is possible to produce a monodisperse break-up of the jet as well as change the droplet size and spacing. These studies resulted in a higher degree of monodispersity as well as a higher production yield.

**Keywords**
Laminar Jet, Break-Up Control, Monodisperse, High-Temperature Process, Fusion Energy

## Introduction

Currently, fusion energy is being developed as a sustainable energy source for future generations. Reactors aim to safely deliver abundant energy from almost inexhaustible sources while producing very limited amounts of long-term radioactive waste (as well as no carbon dioxide). Of the two fuel components, deuterium can be extracted from sea water, while tritium will need to be generated on-site in order to guarantee the self-sufficiency of the reactor, allowing it to operate in a steady-state mode [1].

In order to generate the required tritium, lithium rich ceramic pebbles are to be installed into the wall of the fusion reactor in the form of pebble beds in so-called solid breeder blankets [2]. Upon neutron irradiation (from neutrons generated by the tritium-deuterium reaction in the reactor core), the lithium decays into helium and tritium. The tritium is then extracted from the blanket, processed and rerouted into the reactor core to take part in the fusion reaction, thereby completing the fuel cycle.

Currently, many processes are being developed around the world for the fabrication of the lithium rich ceramic pebbles (for example [3 – 5]). At the Karlsruhe Institute of Technology, a melt-based process named KALOS (Karlsruhe Lithium OrthoSilicate) has been developed, which produces ceramic breeder pebbles consisting of a primary phase of lithium orthosilicate (LOS – $Li_4SiO_4$) with a secondary strengthening phase of lithium metatitanate (LMT – $Li_2TiO_3$) [6, 7]. Synthesis powders are heated in a platinum alloy crucible until a melt is formed, after which a pressure is applied to the system to force the melt through a small nozzle on the underside of the crucible, thereby forming a molten laminar jet. The jet breaks up into droplets which enter a cooling tower where they are solidified, resulting in the formation of pebbles, which are then collected at the base of the tower.

It is important to keep the produced pebbles within the desired size range for the breeding blanket, namely between 250 and 1250 µm, to ease the filling process and to achieve a high packing factor of the pebbles. One of the most important steps of the process, greatly influencing both the yield and the size distribution of the product, is the break-up of the jet. Plateau-Rayleigh instabilities grow on the surface of the jet until the surface tension forces overcome the viscous forces, causing a droplet to break off [8, 9]. In general, random ambient disturbances cause the instability growth, resulting in an irregular break-up of the jet with random droplet sizes and spacings.

Droplets with different momentums are able to catch up to other droplets and coalesce due to the low surface tension, forming larger oversized droplets and ultimately oversized pebbles. It is therefore desired to influence process parameters so as to lead to a stable regular break-up of the jet, resulting in equal droplet sizes and equal spacings between the droplets. In order to quantify the regularity or the stability of the jet break-up, the normalised standard deviation of the droplet spacing is used in this report. This value is also referred to as the coefficient of variation (CV) and can be compared to other experimental set-ups. The lower the number, the more stable and regular the jet break-up is.

In theory, instabilities with a minimum wavelength equal to the jet's circumference will grow on its surface [10]. However, before this discovery was made, Plateau described the presence of an optimum wavelength which will grow the fastest on the jet, thereby supressing other disturbances and leading to a monodisperse break-up [11]. Rayleigh built on Plateau's work and took the jet dynamics into account to mathematically show that the optimum wavelength is roughly 9 times the size of the jet radius [10]. As volume is conserved during the break-up, this results in droplets with a diameter approximately twice the size of the nozzle and jet.

Much work has been carried out to successfully apply desired frequencies to induce the break-up of jets often by using piezo-ceramic oscillators [12 – 15], but also by applying instabilities acoustically to the system [16, 17]. Due to complications caused by the high temperatures involved in the KALOS process, initial tests aimed to control the stability of the jet break-up by controlling the operating pressure and therefore indirectly the speed of the jet. The wavelengths of the instabilities on the surface of the jet were then determined by the jet speed. Later, equipment was developed for applying desired frequencies to the pressure system acoustically and tested at room temperature before being transferred to the KALOS process.

**Material and methods**

In order to obtain recordings of the break-up of the jet, a viewing port was cut in the wall of the oven and a high-speed camera was employed with a telecentric lens. Actively cooled infra-red absorbing glass was placed in the viewing port to protect the lens from the high thermal radiation. To provide sufficient contrast between the jet/droplets and the background, an air cooled block was installed in the oven behind the jet (see Figure 1). By continuously streaming air through the block, the surface was kept at a cooler temperature than all other components in the oven and provided the required contrast for the automatic identification of the jet and droplets in the analysis step. In order to later quantify the break-up of the jet, an image processing algorithm was applied to the high-speed camera recordings [18]. The algorithm automatically resolves the droplets and jet and derives multiple characteristics, which can be used to quantify the jet break-up including the coefficient of variation.

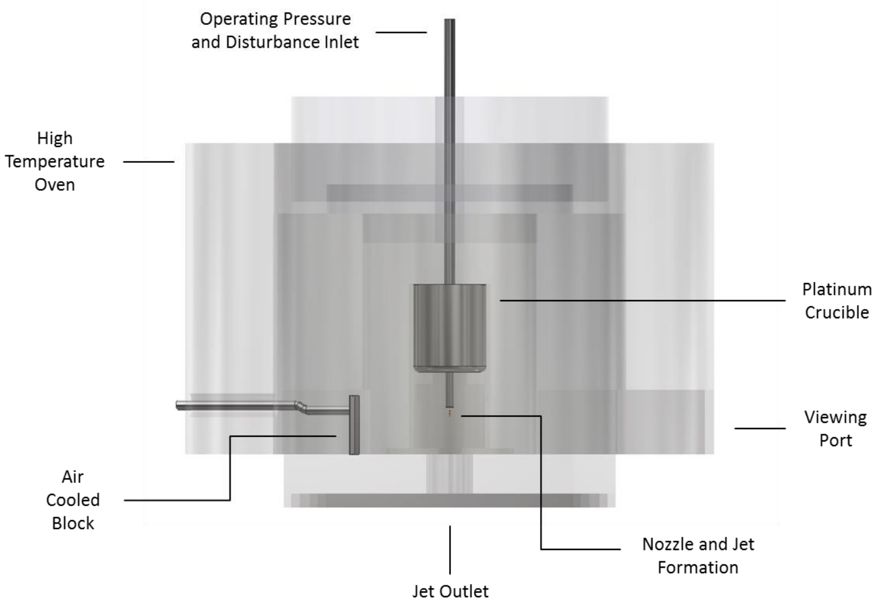


**Figure 1.** High-temperature KALOS production experimental set-up.

In order to test the effects of the operating pressure on the molten jet break-up, a standard batch was prepared. Synthesis powders ($LiOH{\cdot}H_2O$, $SiO_2$ and $TiO_2$), were pre-reacted to form LOS with 30 mol% LMT. The pre-reacted powders were then filled into a platinum alloy crucible and heated up to the processing temperature of 1400 °C to form a melt. A jet was then formed by applying a gas pressure of 400 mbar to the air-tight crucible system via the filling pipe to force the melt through a 300 µm diameter nozzle on the underside (see Figure 1). The pressure was reduced until the jet collapsed, after which the pressure was again increased until a jet was formed at about 60 mbar. Simultaneously, the high-speed camera recording was started (3500 frames per second) and the pressure was increased to 700 mbar. The recording was subsequently evaluated offline using the image processing algorithm. A batch of pebbles was then fabricated using the newly derived optimum operating pressure and the size distribution was determined.

Initial investigations into controlling the break-up of the jet were performed using a replica process set-up at room temperature with a steel crucible and a water-glycerine mix to imitate the melt. A frequency generator consisting of a mid-range speaker and a silicone membrane was developed for applying vertical instabilities directly to the air-tight pressure system within the crucible and was attached at the top of the crucible inlet. A pressure of 70 mbar was used to form a jet through a 300 µm diameter nozzle and then various frequencies from 600 to 1400 Hz were applied to the system while recording with the high-speed camera. Again, the obtained recording was analysed offline.

As the top of the platinum crucible inlet is located outside of the oven and is a cooler part of the air-tight system (T < 100 °C), it was possible to set-up the frequency generator directly in the KALOS process. Additional air cooling was installed to ensure that the device remained at an operational temperature. A standard batch was then prepared as previously described and a pressure of 325 mbar was applied to the system to form a jet on the underside of the crucible. A frequency ramp from 0 – 2000 Hz was then applied to the system while recording with the high-speed camera at 3500 frames per second, after which the recordings were evaluated offline with the image processing algorithm.

## Results and discussion

The effect of the operating pressure on the molten jet stability and the droplet generation frequency can be seen in Figure 2a). According to the theory, at a specific operating pressure, the velocity of the jet will result in the optimum wavelength being applied to the system from ambient disturbances. At 325 mbar, the droplet generation frequency is at its highest, indicating that the optimum wavelength is being applied to the system resulting in the fastest growth of instabilities and leading to the fastest break off of droplets from the jet. At the same operating pressure, the CV value is at its lowest with a value of just above 0.4. These results indicate that the most desirable operating pressure without a controlled excitation of the jet is 325 mbar for generating a stable break-up. The size distribution of the pebbles produced in the subsequently fabricated batch using the determined optimum operating pressure can be seen in Figure 2b). The initial peak is at 625 µm, corresponding well to Rayleigh's theory, which predicts droplets to have roughly twice the diameter as the jet at the optimum driving frequency. It is assumed that any size changes upon solidification of the droplets are negligible and that the jet diameter is approximately equal to the nozzle diameter. However, it can also be seen that many oversized pebbles were formed during the production, which are a consequence of the coalescence of droplets with differing sizes. Still, the fabricated batch had a yield of 90 mass% (pebbles between 250 and 1250 µm).

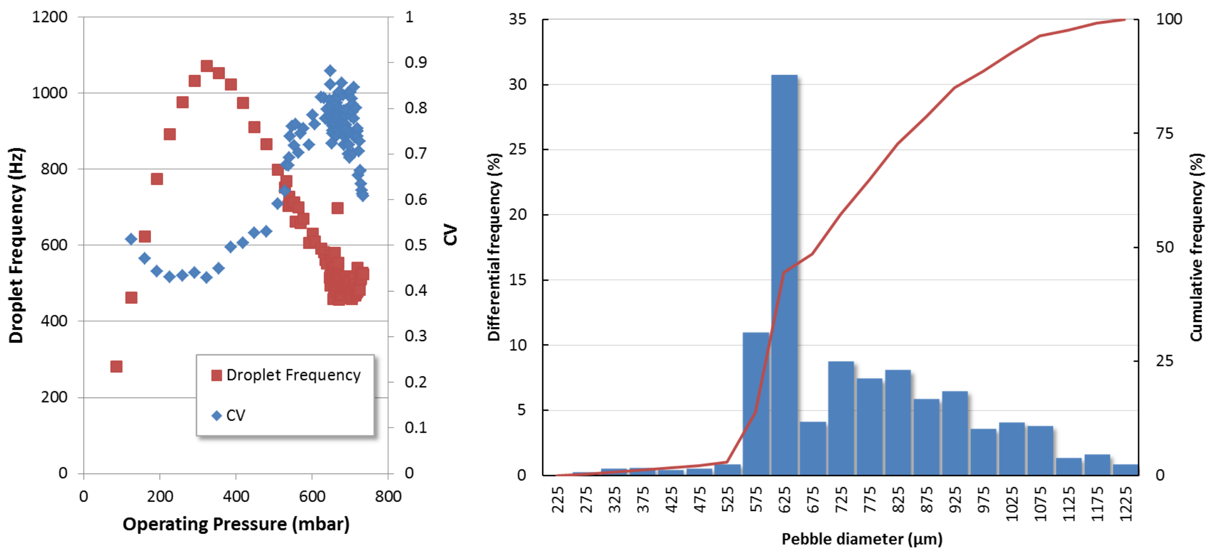


**Figure 2.a)** Effect of the operating pressure on the jet stability and the droplet generation frequency **b)** Size distribution of pebbles produced at 325 mbar.

Figure 3 shows the appearance of the water-glycerine jet with different driving frequencies applied to the system at room temperature. In this case, the operating pressure (and hence the jet velocity) was kept constant, meaning that the only effect on the instability wavelength was the change in the driving frequency. It was found that it was possible to generate a very regular, monodisperse break-up of the jet by applying a frequency of 1042 Hz to the system. It can be seen that all the generated droplets have equal sizes and spacings at this frequency. At 1000 Hz, the break-up of the jet also appears to show a degree of regularity, however many undesirable smaller droplets appear between the main droplets which could be due to the formation of satellite droplets [19, 20]. At all other driving frequencies, almost no differences can be discerned when compared to the jet without any excitation.

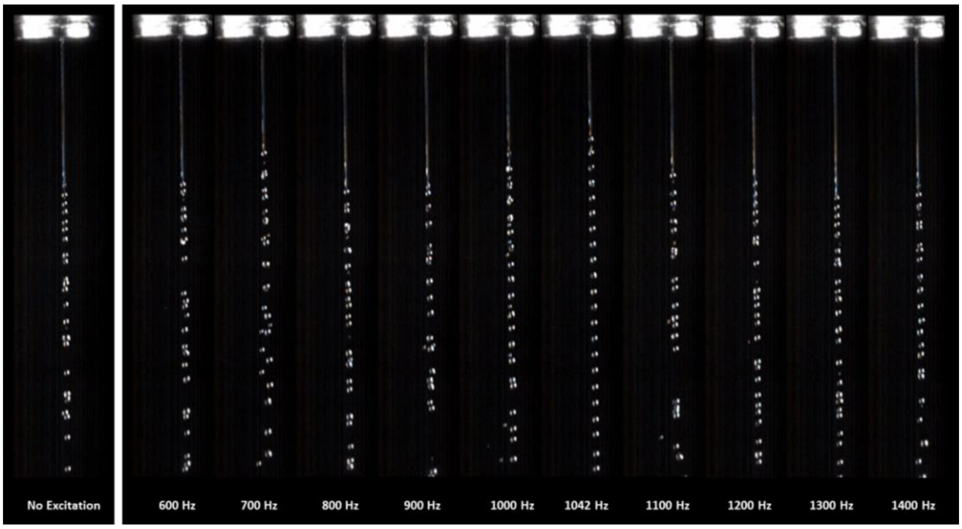


**Figure 3.** Effect of the driving frequency on the appearance of water-glycerine jets with constant velocities.

Figure 4 shows the results computed by the image processing algorithm after being applied to the jets shown in Figure 3. The jet length is defined as the distance from the nozzle to the point where the droplets break off from the jet [21]. This value fluctuates greatly during the break-up of the jet, leading to the use of the average value. The jet length reaches a minimum at approximately 1040 Hz, which agrees with the jet images in Figure 3. The shortest jet length indicates that the optimum wavelength is being applied to the system as the instabilities grow the fastest, causing the jet break-up in the shortest amount of time [22]. These results agree with the effect of the driving frequency on the CV value (also shown in Figure 4), which also shows a minimum amount of variability between the droplet spacings at a frequency of about 1040 Hz.

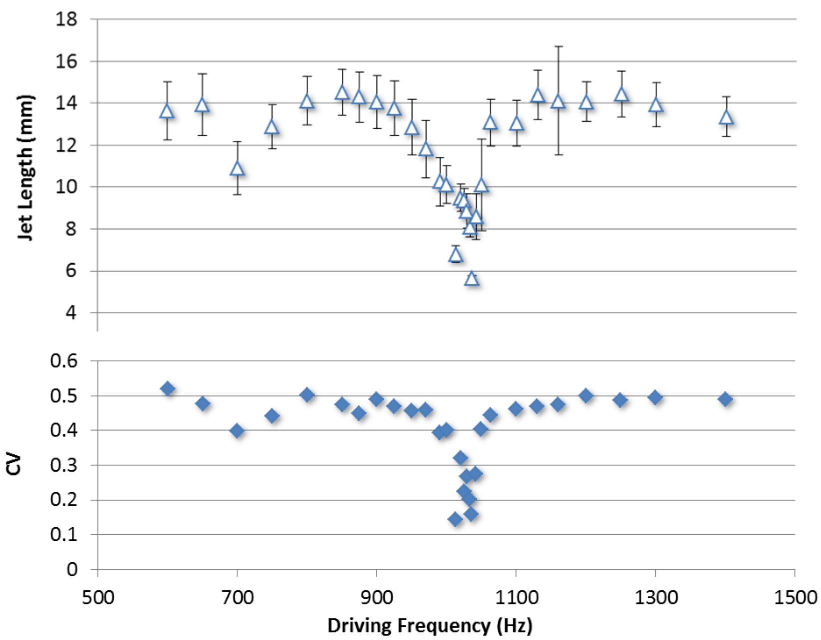


**Figure 4.** Effect of the driving frequency on the jet length and break-up stability for water-glycerine jets.

Figure 5 shows the effect of the driving frequency on the break-up stability of the molten KALOS process jet. It can be seen that the frequency has an effect on the CV value between approximately 400 and 1250 Hz with minimums at about 685 and 900 Hz. Compared to the tests at room temperature, it is clear that the frequency has a larger range of influence for the KALOS process. Between the two minimums, an increase in the CV value can be seen, which is not predicted by Rayleigh's theory. It has been postulated that this could be the effect of resonances within the system as have been detected in similar processes, for example [23]. Further studies will be required to confirm their presence in the KALOS system and how exactly they affect the break-up of the jet.

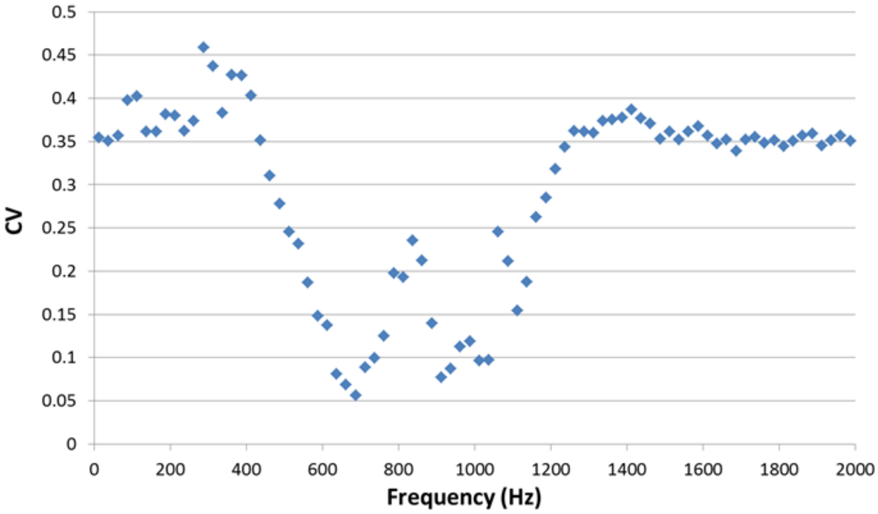


**Figure 5.** Effect of the driving frequency on the break-up stability of the molten jet.

The appearance of the jet at various driving frequencies is shown in Figure 6. The driving frequencies, from which the images were chosen, were selected based on the coefficient of variation values as shown in Figure 5. The jets at 685 and 1025 Hz both have CV values below 0.1 and each shows a highly regular monodisperse break-up. Both the droplet sizes and the spacings between the droplets are extremely even. The jets with driving frequencies of 555, 850 and 1135 Hz have CV values of approximately 0.2. In this case it can be seen that the jets still display a regular break-up when compared to the jet without excitation. However, instances of coalescences are visible (for example at the beginning of the break-up of the 850 Hz jet), which will result in oversized pebbles. When comparing the jets at 685 and 1025 Hz (both with CV values below 0.1), it can also be clearly seen that the driving frequency has an effect on the droplet size and spacing, leading to smaller droplets and spacings with higher frequencies.

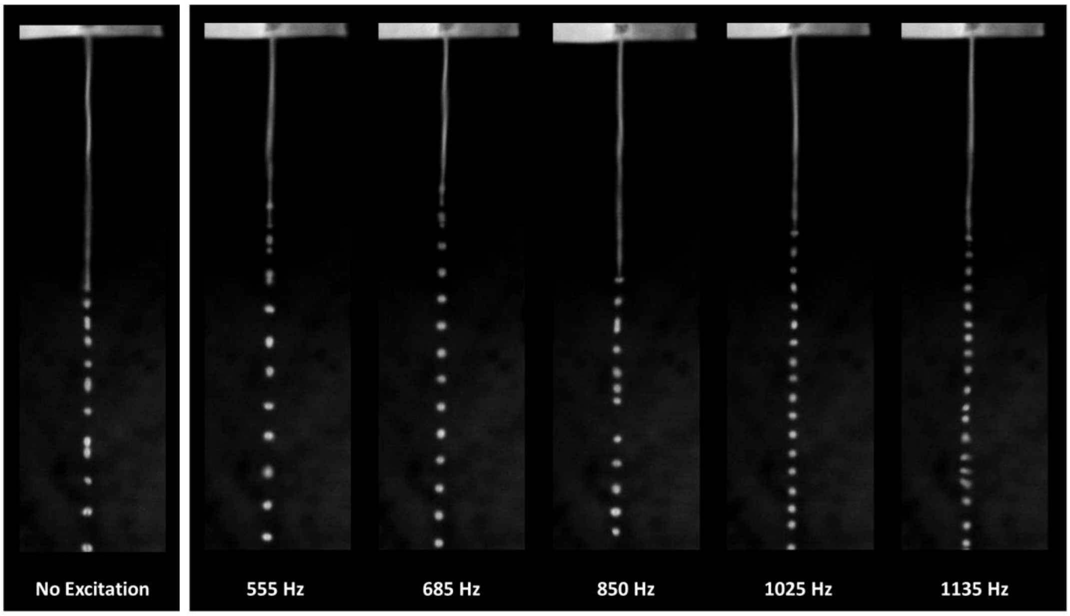

**Figure 6.** Effect of the driving frequency on the appearance of the molten jet.

Figure 7 shows the pebble size distribution of a batch fabricated using a driving frequency of 1070 Hz (which according to Figure 5 results in a CV of approximately 0.1) to induce the jet break-up. An insert of the produced pebbles is also displayed in the figure. It can be seen that almost half the pebbles have a size of 700±50 µm. Again, the initial peak agrees well with Rayleigh's theory. The second peak at 875 µm corresponds to the volume of two coalesced droplets with a diameter of 700 µm. The peaks at 1025 and 1125 correspond to the volume of three and four of the initial droplets respectively. The pebbles with sizes smaller than the first peak can be formed either due to satellite droplets or due to the break-up of droplets due to shear forces below the field of view of the high-speed camera [24]. As the pebble size distribution is highly discrete compared to previously obtained distributions [6, 18, 25], it can be assumed that the droplets being formed are of uniform size when breaking off from the jet. However, other forces within the process, such as turbulence in the cooling tower, result in some extent of droplet coalescence leading to the production of the oversized pebbles. Nevertheless, 94 mass% of the produced pebbles had sizes between 250 and 1250 µm.

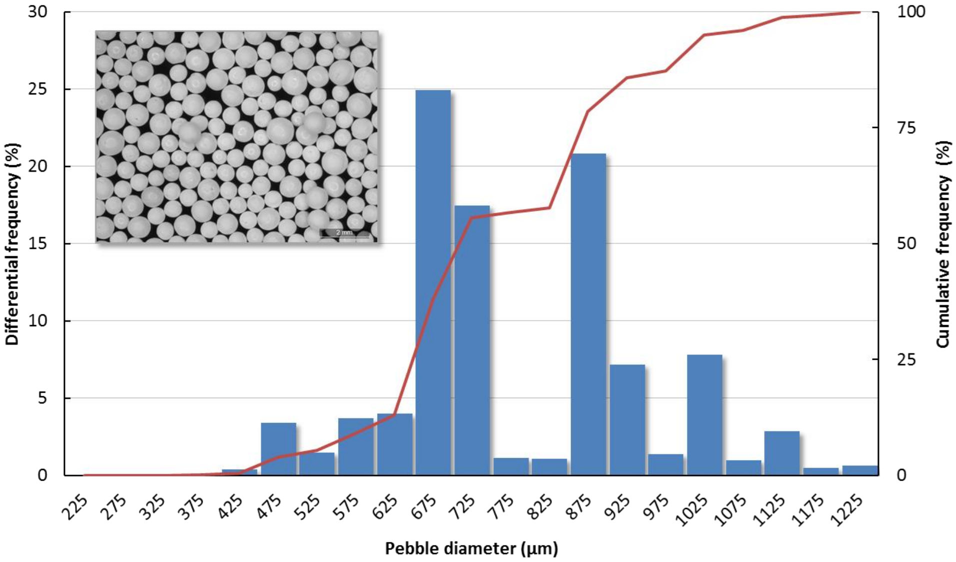


**Figure 7.** Pebble size distribution for a batch fabricated with a driving frequency of 1070 Hz.

**Summary**

Experiments were conducted examining the effects of the operating pressure on the molten jet break-up characteristics of the KALOS process. Following these initial tests, a method for applying desired instabilities acoustically to the air-tight system was developed at room temperature using a steel replica crucible and a water-glycerine mix to imitate the melt. The system was tested and then successfully transferred to the high-temperature process.

In order to quantify the break-up stability, the coefficient of variation was used where lower values indicate less variation between the droplet spacings. By choosing a specific operating pressure, it was possible to reduce the CV of the jet break-up to approximately 0.4. A further reduction was attained by applying selected instabilities to the system, reducing the CV to a minimum of 0.05 with a driving frequency of 685 Hz. In general, all jets with a CV value below 0.1 showed a highly monodisperse break-up. Subsequently, a batch was fabricated using a driving frequency with a corresponding CV value of 0.1 resulting in an increased yield as well as a more discrete size distribution of the product compared to previously fabricated batches. However, oversized pebbles are still being formed, most likely due to droplets coalescing outside the field of view of the camera. Future work will focus on identifying resonances within the high-temperature system and minimising the coalescence of droplets.

**Acknowledgements**

Part of this work leading to this publication received research funding from Fusion for Energy under the Specific Grant Agreement F4E-FPA-380-A3: SG01. This publication reflects the views only of the authors, and Fusion for Energy cannot be held responsible for any use which may be made of the information contained therein.

Part of this work has been carried out within the framework of the EUROfusion Consortium and has received funding from the Euratom research and training programme 2014-2018 and 2019-2020 under grant agreement

No 633053. The views and opinions expressed herein do not necessarily reflect those of the European Commission.

**References**

[1] A. A. Harms, K. F. Schoepf, G. H. Miley and D. R. Kingdon, 2000, 'Principles of Fusion Energy: An Introduction to Fusion Energy for Students of Science and Engineering'
[2] R. Knitter, P. Chaudhuri, Y. J. Feng, T. Hoshino and I. -K. Yu, 2013, J. Nucl. Mater., (442), pp. S420-S424.
[3] J. D. Lulewicz and N. Roux, 2002, J. Nucl. Mater., (307), pp. 803-806.
[4] T. Hoshino and F. Oikawa, 2011, Fusion Eng. Des., (86), pp. 2172-2715.
[5] Y.-H. Park, S. Cho and M.-Y. Ahn, 2014, J. Nucl. Mater., (455), pp. 106-110.
[6] M. Kolb, R. Knitter, U. Kaufmann and D. Mundt, 2011, Fusion Eng. Des., (86), pp. 2148-2151.
[7] R. Knitter, M. Kolb, U. Kaufmann and A. Goraieb, 2013, J. Nucl. Mater., (442), pp. S433-S436.
[8] A. H. Lefebvre and V. G. McDonell, 1989, Atomization and Sprays.
[9] J. Eggers and E. Villermaux, 2008, Rep. Prog. Phys., (71), pp. 1-79.
[10] L. Rayleigh, 1878, P. Lond. Math. Soc., (10), pp. 4-13.
[11] J. Plateau, 1849, Acad. Sci. Brux. Mem., (23).
[12] M. Orme and E. P. Muntz,1990, Phys. Fluids A-Fluid, (7), pp. 1124-1140.
[13] P. Vassallo and N. Ashgriz, 1991, P. R. Soc. A, (433), pp. 269-286.
[14] G. Brenn, F. Durst and C. Tropea, 1996, Part. Part. Syst. Char., (13), pp. 179-185.
[15] W. D. Wu, S. X. Lin and X. D. Chen, 2011, AIChe J, (6), pp. 1386 – 1392.
[16] C. C. Miesse, 1955, Jet Propulsion, (25), pp. 525-530.
[17] W. Debler and D. Yu, 1988, P. Roy. Soc. Lond. A Mat., (415), pp. 107-119.
[18] P. Waibel, J. Matthes, O. Leys, M. Kolb, H. B. Keller and R. Knitter, 2014, Chem. Eng. Technol., (37), pp. 1654-1662.
[19] W. T. Pimbley and H. C. Lee, 1977, IBM J. Res. Dev., (21), pp. 21-30.
[20] W. v. Hoeve, S. Gekle, J. H. Snoeijer, M. Versluis, M. P. Brenner and D. Lohse, 2010, Phys. Fluids, (12), pp. 122003-1-122003-11.
[21] R. P. Grant and S. Middleman, 1966, AIChe J, (4), pp. 669-678.
[22] S. Leroux, C. Dumouchel and M. Ledoux, 1996, Atomization Spray, (6), pp. 623-647.
[23] B. Rollinger and R. Abhari, 2016, Phys. Fluids, (28), p. 074105.
[24] M. Pilch and C. Erdman, 1987, Int. J. Multiphase Flow, (13), pp. 741-757.
[25] O. Leys, P. Waibel, J. Matthes, H. Keller and R. Knitter, 2018, Int. J. Adv. Manuf. Tech., (98), pp. 2311-2318.